Gauge field induced by ripples in graphene

F. Guinea,[1] Baruch Horovitz,[2] and P. Le Doussal[3]
[1]*Instituto de Ciencia de Materiales de Madrid, CSIC, Cantoblanco E-28049 Madrid, Spain*
[2]*Department of Physics, Ben Gurion University, Beer Sheva 84105 Israel*
[3]*CNRS-Laboratoire de Physique Théorique de l'Ecole Normale Supérieure, 24 rue Lhomond, 75231 Cedex 05 Paris, France*
(Received 13 March 2008; revised manuscript received 23 April 2008; published 15 May 2008)

We study the effects of quenched height fluctuations (ripples) in graphene on the density of states (DOS). We show that at strong ripple disorder, a divergence in the DOS can lead to an ordered ground state. We also discuss the formation of dislocations in corrugated systems, buckling effects in suspended samples, and the changes in the Landau levels due to the interplay between a real magnetic field and the gauge potential induced by ripples.

DOI: 10.1103/PhysRevB.77.205421 PACS number(s): 71.23.−k, 71.55.Jv, 72.15.Rn, 73.21.Ac

I. INTRODUCTION

The recent characterization of graphene sheets made up of a single layer of carbon atoms[1,2] has caused great interest. Their unusual electronic band structure and the possibility of tuning the number of electrons lead to a number of interesting features, both from a fundamental perspective and because of its potential applications.[3,4]

The low energy electronic states of graphene are well described, in the continuum limit, by two decoupled two dimensional Dirac equations. The kinetic energy depends linearly on the lattice momentum. The perturbations due to some types of disorder, such as topological lattice defects,[5,6] strains,[7,8] and curvature,[9] enter as an effective gauge field. Curvature, strains, and topological lattice defects are expected to exist in graphene,[10] as experiments show a significant corrugation both in suspended samples,[11] in samples deposited on a substrate,[12,13] and also in samples grown on metallic surfaces.[14]

The statistical properties of the two dimensional Dirac equation in a random gauge field have been extensively studied,[15–19] in relation with the integer quantum Hall effect. It has been shown that the density of states develops a peak at zero energy when the disorder strength exceeds a certain threshold. Furthermore, beyond a second threshold, there is a transition to a glassy phase[20] where the local density of states is dominated by rare regions.[18]

In the following, we will apply the analysis in Ref. 18 to the specific case of graphene, where there are two Dirac equations coupled to the same random gauge field. The model will be detailed in the next section. We analyze in the following section the statistical properties of the gauge field. The main results for the density of states are presented in Sec. IV. Given a divergent density of states at the energy of the Dirac point, we consider the instabilities which may be induced by interactions. Alternative approaches to the interplay between gauge fields and interactions are given in Refs. 21–29, although they did not consider diverging densities of states. Sections VI analyze the related problem of the structural changes which can be induced by the same random strains which give rise to the gauge field, following the analysis in Ref. 24. Section VII discusses a buckling transition in suspended graphene. Section VIII estimates the effects of ripples on density fluctuations in the quantum Hall regime and compares with recent data.[25] The main results of the paper are summarized in Sec. VI.

II. MODEL

We analyze the gauge field induced by the height fluctuations of a graphene layer on a rough substrate. In such case, one expects that the shape of the graphene layer is determined by a competition between the interaction of the layer with the rough substrate, which tends to impose a preferred height, and the elastic properties of the layer. A simple Hamiltonian which models these effects is

$$\mathcal{H} = \mathcal{H}_{subs} + \mathcal{H}_{elastic} + \mathcal{H}_{elec},$$

$$\mathcal{H}_{subs} = \frac{g}{2} \int d^2\vec{r} [h(\vec{r}) - h_0(\vec{r})]^2,$$

$$\mathcal{H}_{elastic} = \frac{\kappa}{2} \int d^2\vec{r} [\nabla^2 h(\vec{r})]^2 + \int d^2\vec{r} \left\{ \frac{\lambda}{2} \left[\sum_i u_{ii}(\vec{r}) \right]^2 + \mu \sum_{ij} [u_{ij}(\vec{r})]^2 \right\},$$

$$\mathcal{H}_{elec} = v_F \int d^2\vec{r} \bar{\Psi}_1(\vec{r}) \{ \sigma_x [-i\partial_x - A_x(\vec{r})] + \sigma_y [-i\partial_y - A_y(\vec{r})] \} \Psi_1(\vec{r}) - v_F \int d^2\vec{r} \bar{\Psi}_2(\vec{r}) \{ \sigma_x [-i\partial_x + A_x(\vec{r})] + \sigma_y [-i\partial_y + A_y(\vec{r})] \} \Psi_2(\vec{r}), \quad (1)$$

where $h(\vec{r})$ is the height of the graphene layer, $h_0(\vec{r})$ is the preferred height which can be assumed to follow closely the substrate height, and $\Psi_1(\vec{r})$ and $\Psi_2(\vec{r})$ are the two inequivalent Dirac (iso)spinors which describe the two inequivalent valleys at the corners of the hexagonal Brillouin lattice. Note that the gauge field couples with opposite signs to the two species of Dirac fermions. The tensor $u_{ij}(\vec{r})$ is the strain tensor associated to the deformation of the graphene layer, given by

$$u_{xx} = \frac{\partial u_x}{\partial x} + \frac{1}{2}\left(\frac{\partial h}{\partial x}\right)^2,$$

$$u_{yy} = \frac{\partial u_y}{\partial y} + \frac{1}{2}\left(\frac{\partial h}{\partial y}\right)^2,$$

$$u_{xy} = \frac{1}{2}\left(\frac{\partial u_x}{\partial y} + \frac{\partial u_y}{\partial x}\right) + \frac{1}{2}\frac{\partial h}{\partial x}\frac{\partial h}{\partial y}. \quad (2)$$

The gauge vector acting on the electrons in Eq. (1) is related to the strain tensor by[26,27]

$$A_x(\vec{r}) = \frac{\beta}{a}[u_{xx}(\vec{r}) - u_{yy}(\vec{r})],$$

$$A_y(\vec{r}) = -2\frac{\beta}{a}u_{xy}(\vec{r}), \quad (3)$$

where $a \approx 1.4$ Å is the length of the bond between neighboring carbon atoms, and $\beta = C\tilde{\beta}$ where C is a constant of order unity and $\tilde{\beta} = -\partial \log(t)/\partial \log(a) \sim 2-3$ is a dimensionless parameter which characterizes the coupling between the Dirac electrons and lattice deformations. Besides the symmetry arguments in Refs. 27, we also assume that the coupling between the electrons and lattice deformations is through the modulation of the hopping between nearest neighbor π orbitals, $t \approx 3$ eV.[28,29] The rest of the parameters which determine the Hamiltonian in Eq. (1) are the electron Fermi velocity, $v_F = 3ta/2$, the bending rigidity, $\kappa \sim 1$ eV, the in-plane elastic constants, $\lambda, \mu \sim 1$ eV Å^{-2}.

In order to model the interaction between the graphene layer and the substrate, we use a simple quadratic expansion around the height $h_0(\vec{r})$ which minimizes the energy in the absence of elastic and electronic energy, parametrized by a coupling g. The value of this parameter is less understood. Estimates based on the analysis of the electrostatic potential between graphene and SiO_2 (Ref. 12) suggest that $g \sim 10^{-2}-10^{-1}$ meV Å^{-4}. By comparing g and κ, one finds that the pinning by the substrate dominates for length scales greater than $l_p \sim (\kappa/g)^{1/4} \sim 10$ Å. The coupling g being strongly relevant, for $l \gg l_p$, it can be considered as effectively infinite and the graphene layer rigidly pinned to the substrate, $h(\vec{r}) \approx h_0(\vec{r})$ for $l \gg l_p$. Note that we assume here that effect of direct pinning of the in-plane modes by the substrate are small and can be neglected.

III. EFFECTIVE GAUGE FIELD

Experiments[13,30] suggest that the height of the graphene layer shows fluctuations of order $h \sim 10$ Å over scales $l \sim 100$ Å. Similar fluctuations have been observed in suspended graphene sheets.[11] We will assume that the effects of the height fluctuations can be described statistically over distances larger than $l_0 \sim 100$ Å. We will then relate the correlations of the effective random gauge field to the (four point) correlations of the (random) height profile $h(\vec{r})$. The calculation is valid whether this profile arises from interaction with a static rough substrate (in which case for $l \gg l_p$ it directly relates to substrate correlations) or from any other mechanism such as in suspended graphene.

An estimate of the magnitude of the effective random gauge field can be obtained by noting that the height change between neighboring lattice points is $\sim a\nabla h$; hence, the distance change is $\sim a(\nabla h)^2$ and the modulation in t is $\delta t \sim \beta t(\nabla h)^2$. Hence, the modulation in A is $\sim \delta t/v_F \sim \beta(\nabla h)^2/a$ which yields an estimate for the variance of the random effective magnetic field $B = [\nabla \times A]_z$:

$$\langle B(q)B(q')\rangle = C_B(q)(2\pi)^2\delta^2(q+q'), \quad (4)$$

$$\pi\sigma = \lim_{q\to 0} q^{-2}C_B(q) \sim \left(\frac{\beta}{a}\right)^2 \int_{|\vec{r}|\le l_0} d^2\vec{r}\left(\frac{h}{l_0}\right)^4 \sim \frac{\beta^2 h^4}{a^2 l_0^2}, \quad (5)$$

where $h \sim 10$ Å is the typical scale of the height fluctuations, as discussed earlier. Typical parameters allow for $\sigma = O(1)$, within range of the transitions that we consider below.

In order to perform a more detailed calculation of the effective gauge field acting on the electrons, we first compute the in-plane displacement field $\vec{u}(\vec{r})$ obtained by minimizing the elastic energy for a given realization of $h(\vec{r})$, and then we estimate the strain tensor $u_{ij}(\vec{r})$. We define

$$f_{ij}(\vec{r}) = \frac{\beta}{a}\frac{\partial h}{\partial x_i}\frac{\partial h}{\partial x_j}. \quad (6)$$

In terms of these quantities, the procedure described above gives for the effective magnetic field acting on the electrons:

$$B(\vec{k}) = ik_y\frac{(3k_x^2 - k_y^2)(\lambda+\mu)}{(\lambda+2\mu)k^4}[k_y^2 f_{xx}(\vec{k}) + k_x^2 f_{yy}(\vec{k}) - 2k_x k_y f_{xy}(\vec{k})]. \quad (7)$$

We assume that the average properties of the height modulations are described by translationally invariant correlation functions, in Fourier:

$$\langle f_{ij}(\vec{q})f_{kl}(\vec{q})\rangle = \mathcal{F}_{ijkl}(q) \quad (8)$$

and are of short range character, i.e., with a finite limit for $ql_0 \ll 1$:

$$\mathcal{F}_{ijkl}(q)|_{q\to 0} = f\delta_{ij}\delta_{kl} + f'(\delta_{ik}\delta_{jl} + \delta_{il}\delta_{jl}), \quad (9)$$

a tensor compatible with the hexagonal symmetry of the lattice parametrized by two dimensionless constants f and f'. Using Eqs. (7)–(9), we find for the correlations (4) of the effective magnetic field at small q:

$$C_B(q) = q^2\left(\frac{\lambda+\mu}{\lambda+2\mu}\right)^2 \sin^2(3\theta)(f+2f'), \quad (10)$$

where $q_x + iq_y = qe^{i\theta}$, where the angle θ is measured from a given lattice axis. The angular dependence of the correlation is consistent with the lattice symmetry; as we show below, only its angular average is relevant for the transitions.

In Eq. (8), we have assumed that the two point function of $(\nabla h)^2$ field has a finite $q=0$ limit. The exact bound $\frac{\beta}{a}|\langle \partial_i h(\vec{r})\partial_j h(\vec{r}')\rangle| \le |\mathcal{F}_{iijj}(\vec{r}-\vec{r})|^{1/2}$ implies that the roughness $h \sim r^\zeta$ of the graphene sheet (hence of the substrate if adsorbed) can be at most $\zeta < 1/2$ in the general case for Eq. (8)

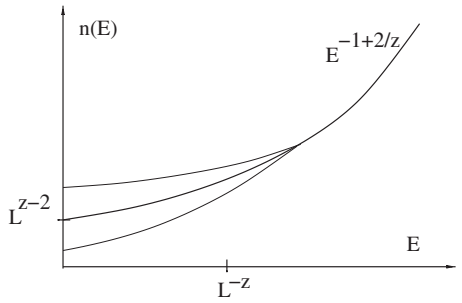

FIG. 1. Sketch of the DOS in a finite size L region for $z<2$. The thick line is a typical value, while the thin line represents the size of fluctuations that are enhanced below the energy L^{-z}. For $z>2$, the DOS increases at small E and its typical value saturates at L^{-2+z}. For $z>3$ (frozen regime), the fluctuations become so strong that the average DOS grows as $L^{-2+\bar{z}}$, where $\bar{z}=1+\sigma>z$. Such finite size fluctuations should be observable in tunneling experiments.

to hold. In a model with Gaussian distributed h, the condition is $\zeta<1/4$ and higher roughness would result in long range (LR) correlations in the disorder. Such LR correlations would presumably arise when quenching thermal fluctuations of a freely fluctuating membrane (which has $\zeta=0.59$, see Ref. 31), although a precise estimate then requires taking into account non Gaussian fluctuations, a nontrivial calculation. Here, we restrict to short range disorder and substrates such that Eq. (7) holds.

IV. ELECTRONIC DENSITY OF STATES

The analysis of the height correlations in the previous section leads us to a model of electrons described by the Dirac equation, in the presence of a gauge field with random correlations. This model is valid at length scales longer that the typical size of the ripples, $l_0 \sim 10^2$ Å, and energies smaller than $W_0 \sim v_F l_0^{-1} \sim 10^{-2}-10^{-1}$ eV.

We analyze the electronic density of states near the Dirac point, $E=0$, using the techniques discussed in Ref. 18. The main difference with the cases considered there is the existence of two Dirac equations coupled to the same gauge field, with couplings of equal absolute value but opposite sign, see $\mathcal{H}_{elec}$ in Eq. (1). The (2+1) dimensional Dirac problem, when projected onto a given energy, becomes a two dimensional problem with excitations with a linear spectrum. Its statistical properties, analyzed within a path integral formalism, are identical to those of quantum bosonic systems in (1+1) dimensions. A derivative of the resulting path integral yields the density of states. The bosonized version of the problem also contains two fields, which become two sets of coupled fields when the replica trick is used to integrate over the disorder. Finally, we make the same variational ansatz as in Ref. 18. The simplest observable is the total density of states (DOS) (see Fig. 1), which is self-averaging and is just twice the DOS of a single Dirac equation (single layer problem as defined in Ref. 18) and behaves as

$$\rho(E) \sim E^{2/z-1}, \tag{11}$$

with

$$z = \begin{cases} 2 - K + \sigma K^2, & \sigma < 2/K^2 \\ K(\sqrt{8\sigma} - 1), & \sigma > 2/K^2, \end{cases} \tag{12}$$

where K is a parameter which describes the kinetic energy of the field in the bosonized version of the model and, for the noninteracting case which corresponds to the Hamiltonian in Eq. (1), takes the value $K=1$. The parameter σ determining the exponent in Eq. (12) is found to be given by the angle average of Eq. (10):

$$\sigma = \frac{1}{2\pi}\left(\frac{\lambda+\mu}{\lambda+2\mu}\right)^2 (f+2f'), \tag{13}$$

i.e., the strength of the random Gauge field, consistent with the order of magnitude estimate (5).

The change in the dependence of the exponent z on the strength of the gauge field, σ, in Eq. (12) is associated with a phase transition in the disordered bosonic model. For $\sigma > \sigma_c = 2/K^2$, the local DOS (averaged over regions of size up to $L \sim |E|^{-1/z}$) exhibits strong fluctuations and non-Gaussian tails (i.e., its disorder average being different from its typical value) due to the dominance of rare regions. Note that the divergence of the DOS at $E=0$ occurs at $\sigma = 1/K^2 < \sigma_c$, i.e., before the freezing transition in the one layer problem as disorder is increased.

The effect on the DOS of an additional smooth random scalar potential with variance δ, corresponding to local fluctuations of the chemical potential, induced by, e.g., the substrate, has been discussed in Ref. 18. It leads to

$$\rho(E) = E^{2/z-1}\mathcal{R}(E/\delta^{z/z'}), \tag{14}$$

where the exponent z' is given by

$$z' = \begin{cases} 2 - 2K + 4\sigma K^2, & \sigma < \dfrac{1}{2K^2} \\ 2K(\sqrt{8\sigma} - 1), & \sigma > \dfrac{1}{2K^2} \end{cases} \tag{15}$$

and exhibits a transition at $\sigma_c' = 1/(2K^2) = \sigma_c/4$. This leads to a finite and nonzero DOS at zero energy:

$$\rho(E) \sim \delta^{(2-z)/z'}, \tag{16}$$

a behavior which thus exhibits two distinct freezing transitions. The divergence of the DOS at $\sigma=1$ (for $K=1$) is in between these transitions.

Although we will not study this aspect in detail here, it is also interesting to note that since the two Dirac equations describing the two valleys (the two Fermi points) feel opposite random gauge fields, mutual correlations of the local DOS in the two valleys as measured by $\langle \rho_1(E,r)\rho_2(E,r)\rangle^c$ are strong. They are found to exhibit a transition at a different value of disorder $\sigma = 1/(2K^2)$ as can be seen by a study analogous to the two layer model of Sec. IV B of Ref. 18.

V. INTERACTION EFFECTS AND ELECTRONIC INSTABILITIES

For sufficiently large disorder, $\sigma>1$, the density of states, and, as a consequence, the electronic compressibility, di-

verges at $E=0$. The electron-electron interaction, or the interaction of the electrons with other degrees of freedom, will lead to instabilities, which suppress the compressibility.

Within mean field theory, the effects of interactions on the electronic band structure can be described as an external potential which must be calculated self-consistently. A simple such potential which opens a gap at $E=0$ is the shift of the energy on one sublattice of the honeycomb structure with respect to the other. This shift can be associated with a spin or with a charge density wave, or it can be induced by phonons[32] or by short range electron-electron interactions.[33–36] In the continuum model described here, it enters as a mass term:

$$\mathcal{H}_{elec}^{tot} = \mathcal{H}_{elec} + \mathcal{H}_{\Delta},$$

$$\mathcal{H}_{\Delta} = \Delta \sum_i \int d^2\vec{r} [\bar{\Psi}_i(\vec{r}) \sigma_z \Psi_i(\vec{r})], \tag{17}$$

where $\mathcal{H}_{elec}$ is defined in Eq. (1). The total electronic hamiltonian satisfies

$$(\mathcal{H}_{elec} + \mathcal{H}_{\Delta})^2 = (\mathcal{H}_{elec})^2 + \Delta^2 \mathcal{I}, \tag{18}$$

where $\mathcal{I}$ is the two dimensional unit matrix, independent of spatial position, which acts on the space spanned by the four component electronic (iso)spinors (note that we consider the two valleys separately). The eigenvalues of the electronic Hamiltonian satisfy $\epsilon_n^{tot^2} = \epsilon_n^2 + \Delta^2$, where ϵ_n is an eigenvalue of $\mathcal{H}_{elec}$. As a result, the density of states associated with $\mathcal{H}_{elec}^{tot}$, $\rho_{\Delta}(E)$ satisfies

$$\rho_{\Delta}(E) = \frac{E}{\sqrt{E^2 - \Delta^2}} \rho(\sqrt{E^2 - \Delta^2}), \tag{19}$$

and, using the expression in Eq. (11), we find

$$\rho_{\Delta}(E) = \begin{cases} 0, & |E| < \Delta \\ \dfrac{1}{l_0^2} \dfrac{E(\sqrt{E^2 - \Delta^2})^{2/z-2}}{W_0^{2/z}}, & W_0 > |E| > \Delta, \end{cases} \tag{20}$$

where the energy scale $W_0 = v_F/l_0$ is inserted so that for $E \gg W_0 \gg \Delta$ the value of $\rho_{\Delta}(E)$ crosses over into the density of states of the clean system, $\rho(E) \sim |E|/v_F^2$.

The self-consistent value of Δ is determined by the competition between the cost in energy associated with the formation of the gap and the decrease in electronic energy due to the reduction in the density of states at the Fermi level. Near the transition, Δ is small compared to the other energy scales of the model, and the energy required to create the charge or spin density wave can be expanded as function of Δ. For simplicity, we assume that the ordered phase is a spin density wave induced by the on-site Hubbard repulsion U which breaks the sublattice symmetry and produces a gap $\Delta = US/2$, where S is the resulting polarization per site. The total free energy is the sum of the kinetic energy and the gain in interaction energy obtained by inducing the polarization:

$$F_{tot} = F_{elec} + F_{SDW},$$

$$F_{SDW} = \frac{\Delta^2}{U},$$

$$F_{elec} = -4Ta^2 \int_{\Delta}^{W_0} [\ln(1 + e^{(-E-E_F)/T}) + \ln(1 + e^{(E-E_F)/T})] \rho_{\Delta}(E) dE, \tag{21}$$

where 4 allows for spin and valley degeneracy and we allow for a possibly nonzero Fermi energy E_F. The induced gap is given by minimizing the total free energy and with a change of integration variable:

$$1 = 2a^2 U \int_0^{W_0} \frac{\sinh(\sqrt{E^2 + \Delta^2}/T)}{\cosh(E_F/T) + \cosh(\sqrt{E^2 + \Delta^2}/T)} \frac{\rho(E) dE}{\sqrt{E^2 + \Delta^2}}. \tag{22}$$

We consider first the case $E_F = T = 0$, where $F_{elec} \to E_{elec} = -4a^2 \int_{\Delta}^{W_0} E \rho_{\Delta}(E) dE$. The integrand can be expanded for $E \gg \Delta$, where it goes as $\Delta^2 E^{(2/z)-2}$. As a result, we obtain a contribution to the electronic energy $\delta_1 E_{elec}(\Delta) \sim -(a/l_0)^2 \Delta^2 / W_0$. There is also a contribution from the region $E \sim \Delta$. This term in $E_{elec}(\Delta)$ can be written as $\delta_2 E_{elec}(\Delta) \sim -(a/l_0)^2 \Delta^{(2/z)+1} W_0^{-2/z}$.

The relative strength of F_{SDW} and F_{elec} discussed above leads to the existence of three regimes: (i) $2/z - 1 > 0$. The electronic energy is determined by $\delta_1 E_{elec}(\Delta)$. Both the magnetic and electronic energies go as $\sim \Delta^2$, and, for $U \ll v_F/a$, the minimum energy is at $\Delta = 0$. (ii) For $2/z - 1 = 0$, we find $\delta_1 E_{elec} \sim -2(a/l_0)^2 \Delta^2 / W_0 \log(W_0/\Delta)$. The magnetic energy is greater by a logarithmic factor, and there is an ordered phase, with $\Delta \sim W_0 e^{-(W_0 l_0^2)/(2Ua^2)}$. The problem becomes equivalent to the Peierls analysis of the instability of a one dimensional metal. (iii) For $2/z - 1 < 0$, the leading contribution is $\delta_2 E_{elec}$. There is a magnetic phase with a gap

$$\Delta_c \sim W_0 \left(\frac{a^2 U}{l_0^2 W_0} \right)^{z/(z-2)}. \tag{23}$$

We now analyze the way in which the magnetic phase which always exists for $2/z - 1 < 0$ is modified when $E_F, T \neq 0$. In particular, the order of the transition is determined by the sign of the a_4 coefficient in the free energy expansion $F = a_2 \Delta^2 + a_4 \Delta^4$. Taking a $\partial_{\Delta^2}|_0$ on the right hand side of Eq. (22) yields a_4; hence, the simultaneous conditions $a_2 = 0$ and $a_4 = 0$ determine a critical E_F, with $E_F^c = \alpha(z) T_c$ whenever $T_c \ll W_0$, such that the transition changes from second order for $E_F < E_F^c$ to first order in the region $E_F > E_F^c$, where we have $a_4 < 0$. We find numerically that $\cosh \alpha(z)$ varies between 3.4 at $z=2$ and 2 at $z \to \infty$.

A typical phase diagram with $z > 2$ is shown in Fig. 2, where the value of the gap Δ_c at the critical temperature, in the region where the transition is first order, is also shown. When the line of first order transitions is crossed, the electron density jumps discontinuously. For sufficiently large values of E_F, we find that $\Delta_c(E_F) > E_F$. When the transition line is crossed in this region, the electron density in the ordered phase is zero. The phase diagram as function of temperature and electron density is shown in Fig. 3.

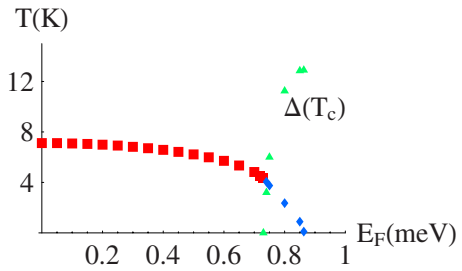

FIG. 2. (Color online) Critical temperature as function of chemical potential. The parameters used are $W_0=200$ meV, $l_0=10a$, $\sigma=1.4$ ($z=2.4$), and $U=1$ eV. The value of σ implies an average height fluctuation $h\approx 3.4$ Å. The blue diamonds give the critical temperature when the transition is discontinuous. The green triangles are the values of the gap Δ, in Kelvin, at the transition temperature, in the region where Δ jumps discontinuously from zero to a finite value.

VI. FORMATION OF LATTICE DEFECTS

A. Unbinding of dislocations

As discussed earlier, ripples, e.g., due pinning to a rough substrate, induce in-plane strains. If these strains are sufficiently large, it will become favorable to relax them by creating lattice dislocations. It is convenient to view the out-of-plane deformations as inducing quenched random stresses coupling linearly to the in-plane strain tensor $\tilde{u}_{ij}$ via an energy density $\Sigma_{ij}\sigma_{ij}\tilde{u}_{ij}$. One can then apply the result of Ref. 24 for the threshold beyond which random stresses generate dislocations.

Using Eq. (1), the random stress tensor field which renormalizes the fugacity of dislocations is

$$\sigma_{xx}=\frac{\lambda}{2}\left[\left(\frac{\partial h}{\partial x}\right)^2+\left(\frac{\partial h}{\partial y}\right)^2\right]+\mu\left(\frac{\partial h}{\partial x}\right)^2,$$

$$\sigma_{yy}=\frac{\lambda}{2}\left[\left(\frac{\partial h}{\partial x}\right)^2+\left(\frac{\partial h}{\partial y}\right)^2\right]+\mu\left(\frac{\partial h}{\partial y}\right)^2,$$

$$\sigma_{xy}=\mu\frac{\partial h}{\partial x}\frac{\partial h}{\partial y}. \tag{24}$$

We assume that the correlations of this field are given by

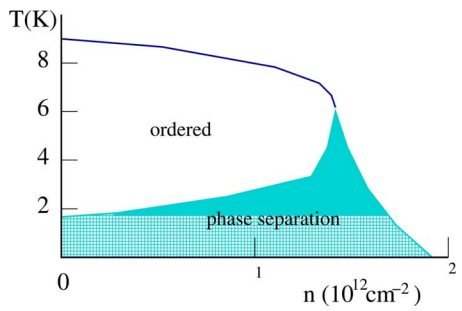

FIG. 3. (Color online) Approximate phase diagram as function of electron density and temperature, obtained with the same parameters used in Fig. 2 The existence of a first order transition leads to a region where electronic phase separation is induced.

$$\langle\sigma_{ij}(\vec{q})\sigma_{kl}(-\vec{q})\rangle|_{q\to 0}=[\sigma_\lambda\delta_{ij}\delta_{kl}+\sigma_\mu(\delta_{ik}\delta_{lj}+\delta_{il}\delta_{jk})], \tag{25}$$

where the parameters σ_μ and $\sigma_\lambda+2\sigma_\mu$ measure the strength of random shear stresses and compressional stresses, respectively.

In presence of random stresses, an isolated dislocation in a region of size L feels a random potential whose minima grow typically $\sim -\ln L$. The logarithmic elastic energy cost of creating a dislocation can then be overcome, and thus dislocations will proliferate at $T=0$ when

$$\tilde{\sigma}=\frac{\lambda(\lambda+2\mu)\sigma_\mu+\mu^2(\sigma_\lambda+2\sigma_\mu)}{\mu^2(\lambda+\mu)^2}\geqslant\tilde{\sigma}_c=\frac{a^2}{16\pi}, \tag{26}$$

where we have neglected the effect of screening of the elastic coefficients by disorder, which have been shown to be small[37]). To the same accuracy, this formula holds for all $T<T_m/2$ where $T_m=K_0a^2/(16\pi)$ is the melting temperature of a pure $2d$ crystal associated to the unbinding of dislocations,[38] with $K_0=4\mu(\mu+\lambda)/(\mu+2\lambda)$, while the threshold decreases as $\tilde{\sigma}_c(T)=4\tilde{\sigma}_c\frac{T}{T_m}(1-\frac{T}{T_m})$ at higher T. For $\tilde{\sigma}>\tilde{\sigma}_c$ and at $T=0$, the scale L above which dislocation first appear can be estimated as in Ref. 39 and corresponds to the total energy cost $\frac{K_0a^2}{8\pi}(1-\sqrt{\tilde{\sigma}/\tilde{\sigma}_c})\ln(L/l_0)+E_c$ becoming negative. We have taken into account the dislocation core energy $E_c=E_c^0+\frac{K_0a^2}{8\pi}\ln(l_0/a)$ at scale l_0 (E_c^0 denotes the bare core energy). Because of logarithms, this scale can be large; hence, it can alternatively be viewed as defining an effective size dependent threshold $\tilde{\sigma}_c(L)$. The dislocation density above this scale can be estimated by arguments similar to Ref. 40.

The quantities σ_λ and σ_μ can be written in terms of the correlations of the function f_{ij}, given in Eqs. (8) and (3):

$$\sigma_\lambda=\frac{a^2}{\beta^2}[\mu^2(f+2f')+\lambda(\lambda+2\mu)(f+f')],$$

$$\sigma_\mu=\frac{a^2}{\beta^2}\mu^2f'. \tag{27}$$

Inserting this result in Eq. (26), and assuming that $\beta,\lambda/\mu\sim O(1)$, we find that dislocations will proliferate when the height correlations are such that $h^2/(l_0a)\gtrsim 1$, which is the same combination of scales which determines the existence of a divergence in the electronic density of states.

B. Buckling into the third dimension

An effect not taken into account above is that dislocations may buckle in the third dimension to lower their energy. For a free membrane (in the absence of a substrate), this occurs for scales larger than the buckling radius R_b, and below that scale the membrane remains flat and Coulomb gas logarithmic scaling holds. In principle, for a free membrane in the presence of internal in-plane random stresses, if R_b is large enough [values such as $R_b\sim 10^2\kappa/(K_0a)$ are quoted in Ref. 41], i.e., if $R_b>l_0\gg a$, the above energy estimate setting $L=R_b$ can be used to determine the disorder threshold at which

buckled dislocations would occur. However, if one takes into account the pinning of the height field to the substrate, the energy calculation of Ref. 41 remains valid for scales smaller than l_p but must be reexamined for scales larger than l_p, a problem left for future study.

C. Gauge fields associated with dislocations

Note, finally, that dislocation cores act on the electrons outside the core as vortices[34] of flux $\Phi=\epsilon\Phi_0/3$, where Φ_0 is the quantum unit of flux ($=2\pi$ in our units) and $\epsilon=\pm 1$. Hence, the existence of dislocations will increase the random field due to elastic strains considered so far. Given a set of dislocations at position $\vec{r}_n$ and Burgers charges $\vec{b}_n$, the resulting effective magnetic field can be written $B(\vec{r})=(\Phi_0/3)n(\vec{r})$, where $n(\vec{r})=\Sigma_n\epsilon_n\delta(\vec{r}-\vec{r}_n)$ and the signs are given by $\epsilon=2\vec{b}\cdot a_1 \bmod 2\pi$. If positions and signs were chosen uncorrelated (such as in a quench from infinite temperature), it would result in a LR correlated random gauge field, i.e., $C_B(q)\sim\Phi_0^2 d^{-2}$ at small q in Eq. (4), where d is the mean distance between defects.[42]

This procedure, however, leads to Burgers charge fluctuations growing as $\pm\sim L$ in an area L^2, hence a very large elastic energy, $L\ln L$. If the system can relax, this energy is screened and the result is a finite parameter σ as defined in Eq. (5). In cases where the dislocation density is not very small, it can be estimated from a Debye-Hückel theory. One nonequilibrium example is a quench of a pure crystal from a (moderate) temperature $T_Q>T_m$ to low temperature in which case $\langle n(\vec{q})n(-\vec{q})\rangle=T_Q q^2/(E_c^0 q^2+K_0 a^2)$; hence, $\sigma=T_Q\Phi_0^2/(9\pi K_0 a^2)$. Further relaxation of $\sim\ln L$ energy would then occur. Another example is the distribution of dislocations induced by the ripples as in Eq. (26), with $\tilde{\sigma}>\tilde{\sigma}_c$. Then one estimates[43] $\langle n(\vec{q})n(-\vec{q})\rangle=\frac{1}{4}q^2\tilde{\sigma}K_0^2 a^2/(E_c^0 q^2+K_0 a^2)^2$; hence, $\sigma=\tilde{\sigma}\Phi_0^2/(36\pi a^2)$. Very near the transition, Debye-Hückel does not apply as σ vanishes at σ_c proportionally to the density of dislocations.

VII. RIPPLES IN SUSPENDED GRAPHENE

Finally, we discuss a possible source for ripples in suspended graphene.[11,44,45] Upon etching a preexisting rough substrate, the rippled graphene sheet would tend to relax to a flat configuration with higher projected area. This, however, may be precluded if the sheet is pinned at its boundaries. Indeed, it is known that fixed connectivity membranes exhibit a buckled state when constrained at their boundaries by a fixed frame of projected area A_f smaller than the equilibrium area of the unconstrained membrane A. As discussed in Ref. 46 it results in an additional compressional energy term of the form $\tau\int d^2\vec{r}\Sigma_i u_{ii}$ and hence implies that the energy of flexural modes becomes, to lowest order, $\frac{1}{2}\int d^2\vec{r}[\kappa(\nabla^2 h)^2+\tau(\nabla h)^2]$. In the buckled phase, $A_f<A$, $\tau<0$, an instability thus develops at scales larger than $\xi_h\sim(\kappa/|\tau|)^{1/2}$. This phase can be described as a nonhomogeneous mixture of pure flat phases with different orientations. For arbitrary boundary conditions, it is expected to be nontrivial since, contrary to a one dimensional rod; in a polymerized membrane, the in-plane modes cannot fully relax the flexural constraints, i.e., the transverse part of the flexural strain tensor, $P_{ij}^T(\nabla)(\partial_i h\partial_j h)$, cannot be relaxed by the in-plane strain field. While demonstrating the instability is simple, the full calculation of the resulting shape requires consideration of nonlinear terms and is difficult. The problem of relaxation from a randomly rippled configuration with a fixed frame constraint deserves further study, in particular, the question of whether there is some memory of the initial ripple pattern.[47]

Note that one may consider, alternatively, unconstrained boundary and apply a tension $-f\int d^2\vec{r}\partial_i u_i$. The buckling transition[46] has been mostly studied on the side where the sheet is stretched (the effective $\tau_R\to 0^+$). It was found that $(A_f-A)/A\sim\tau_R\sim|f|^{1/\delta}\mathrm{sgn}(f)$ and the correlation lengths $\xi_h\sim\xi_u\sim|f|^{-\nu/\delta}$ for flexural and phonon modes at small f. While entropic effects produce nontrivial values for these exponents, these may be observable only at large scales, and at intermediate scales mean field values $\delta=1$, $\nu=1/2$ (discussed above) are appropriate. It would thus be interesting to study the other side of this transition.

VIII. BROADENING OF LANDAU LEVELS IN THE PRESENCE OF A REAL MAGNETIC FIELD

In the presence of a real magnetic field B, we expect that the Landau levels will be broadened by the effective field B_{rip} due to the ripples. Alternatively, the local electronic density corresponding to N full Landau levels is fluctuating according to $n(\mathbf{r})=[B+B_{rip}(\mathbf{r})]N/\phi_0$, where ϕ_0 is the flux quantum. Such density fluctuations were recently measured[25] showing $\delta n=\pm 2.3\times 10^{11}\ \mathrm{cm}^{-2}$ at a field of $11T$ for $N=2,6,10$. In this section, we estimate the contribution of the random gauge field due to ripples to these density fluctuations.

Consider the density n measured on a length scale L, and its probability distribution, near an average density $\underline{BN/\phi_0}$. We express the energies of these levels as $\epsilon_N=v_F\sqrt{2e}\sqrt{\underline{BN'}}$ with $N=4N'+2$, and $\underline{N'=0,\pm 1,\pm 2,\ldots}$. We assume first $l_0>l_B\sqrt{N}$, where $l_B=\sqrt{\phi_0/(2\pi B)}$ is the cyclotron radius and $l_B\sqrt{N'}$ estimates the size of an orbit in the Nth Landau level. Each Landau orbit has then a random shift $\pm B_{rip}(\mathbf{r})$, where the $\pm$ corresponds to the K and K' valleys that feel opposite gauge fields. The density distribution is

$$P(n)=\int_{r<L}\sum_{\pm}\delta(n-BN/\phi_0\pm B_{rip}(r)N/\phi_0)d^2r/2L^2. \tag{28}$$

The average is $\langle n\rangle=BN/\phi_0$ while the variance is

$$\langle\delta n^2\rangle=\frac{N^2}{\phi_0^2L^4}\left\langle\left[\int_{r<L}B_{rip}(\mathbf{r})d^2r\right]^2\right\rangle=\frac{N^2}{4\pi^2L^4}\left\langle\left[\oint A(u)du\right]^2\right\rangle, \tag{29}$$

where $B_{rip}=[\nabla\times A]_z\phi_0/2\pi$ and A is the random gauge field considered in the previous Sections (with the appropriate change in units) and the contour enclose the area of measurement. To estimate the variance in Eq. (29), we use Eq. (5)

with a cutoff $\exp(-q^2 l_0^2/2)$. In real space, it corresponds to $\langle A_i(\mathbf{r})A_j(\mathbf{r})\rangle \sim (\sigma/2l_0^2)\exp[-(\mathbf{r}-\mathbf{r}')^2/2l_0^2]$, where we neglect[48] the transversality constraint on A. It yields

$$\langle \delta n^2 \rangle_L \approx \frac{N^2 \sigma}{4\pi l_0 L^3}. \tag{30}$$

The experimentally more relevant case is $l_0 < l_B\sqrt{N}$. In this case, we argue that $\mathbf{A}(\mathbf{r})$ can be replaced by its average within a Landau state, so that an average ripple field is

$$B_{av}(\mathbf{r}) = \frac{1}{2\pi N l_B^2} \int d^2 r_0 B_{rip}(\mathbf{r}_0) e^{-(\mathbf{r}-\mathbf{r}_0)^2/2Nl_B^2} \tag{31}$$

and its Fourier transform is $B_{av}(q) = B_{rip}(q)\exp(-q^2 N l_B^2/2)$. This replaces $l_0 \to l_B\sqrt{N}$ in Eq. (30), and identifying L with the tip size l_{tip} in the experiment,[25] we obtain

$$\langle \delta n^2 \rangle_L \approx N^{3/2} \frac{\sigma}{4\pi l_B l_{tip}^3}. \tag{32}$$

Using[25] $l_0 \approx 100$ nm and $l_B \approx 10$ nm, Eq. (32) yields numbers consistent with the experiment, except for the N dependence. Note that an even weaker dependence in N ($\delta n \sim N^{1/4}$) is obtained if one assumes that $L = l_B\sqrt{N}$ is the only averaging scale.

It is also interesting to estimate the energy broadening $\delta\epsilon_N$ of the Landau levels, which in the absence of ripples have energies $\epsilon_N = v_F\sqrt{2e}\sqrt{BN'}$, with $N = 4N' + 2$. The field associated with the ripples changes locally the energy of the Landau levels, which become $\epsilon_N = v_F\sqrt{2e}\sqrt{(B \pm \delta B_{rip})N'}$, where δB_{rip} is the average value of B_{rip} in the region occupied by the Landau level. A calculation based on Eq. (30) with $L = l_B\sqrt{N}$ then yields the estimate for $N > 2$,

$$\delta\epsilon_{N'} \approx v_F \left(\frac{\sigma}{8 l_0 l_B}\right)^{1/2} N^{-1/4}, \tag{33}$$

in the regime $l_B\sqrt{N} > l_0$.

Finally, we note that the $N' = 0$ level has no broadening at all. This remarkable result is obtained by factorizing the $N' = 0$ eigenstates of the free Dirac system in a magnetic field with the well known zero energy solutions of the random gauge problem.[15,18] This set has the proper Landau degeneracy and is therefore an exact solution for the zero energy Landau level with random gauge.

IX. CONCLUSIONS

We have analyzed the effect of random gauge fields on the electronic structure of corrugated graphene. We find that the local density of states diverges at the Dirac energy $E = 0$ as $\rho(E) \propto E^{2/z-1}$, with $z > 2$, for sufficiently strong disorder. The scale of height fluctuations, h, should satisfy $\beta h^2/(la) \gtrsim 1$, where $\beta \sim 1-2$ gives the coupling between the electrons and the lattice strains, l is the typical spatial scale of the disorder, and a is the lattice constant.

A divergence in the density of noninteracting density of states implies the existence of instabilities in the presence of electron-electron interactions. We have analyzed the possibility that a gap will open at low temperatures, depleting the low energy density of states. We have found a first order transition to an ordered state at large E_F. This discontinuous transition, in turn, implies electronic phase separation.

When the strains which induce the gauge potential are sufficiently strong, they can lead to an instability and the formation of lattice dislocations. This change takes place for $C(\lambda, \mu)h^2/(la) \gtrsim 1$, where $C(\lambda, \mu) \sim 1$ is a dimensionless parameter which depends on the elastic constants of the material.

We have described the main features of the buckling instability which may arise in suspended systems under compression. Finally, we analyze the changes induced in the Landau levels induced by a magnetic field by the gauge potential associated to ripples and show correspondence with experimental data.[25]

Our analysis is consistent with previous work on the changes in the electronic density of states in graphene in the presence of ripples[49] (see also Ref. 50). A transition to a state magnetically ordered in highly disordered systems agrees with the observation of magnetism in irradiated graphite samples.[51] The existence of charge inhomogeneities, due to electronic phase separation, can help explain the observation of charge puddles when the Fermi energy is close to the Dirac energy.[25]

ACKNOWLEDGMENTS

This work was supported by MEC (Spain) through Grant No. FIS2005-05478-C02-01, the Comunidad de Madrid, through the program CITECNOMIK, CM2006-S-0505-ESP-0337, the European Union Contract No. 12881 (NEST), ANR Program No. 05-BLAN-0099-01, and the DIP German Israeli program. B.H. and F.G. thank the Ecole Normale Supérieure for hospitality and for support during part of this work.

[1] K. S. Novoselov, A. K. Geim, S. V. Morozov, D. Jiang, Y. Zhang, S. V. Dubonos, I. V. Gregorieva, and A. A. Firsov, Science **306**, 666 (2004).

[2] K. S. Novoselov, D. Jiang, F. Schedin, T. J. Booth, V. V. Khotkevich, S. V. Morozov, and A. K. Geim, Proc. Natl. Acad. Sci. U.S.A. **102**, 10451 (2005).

[3] A. K. Geim and K. S. Novoselov, Nat. Mater. **6**, 183 (2007).

[4] A. H. Castro Neto, F. Guinea, N. M. R. Peres, K. S. Novoselov, and A. K. Geim, arXiv:0709.1163, Rev. Mod. Phys. (to be published).

[5] J. González, F. Guinea, and M. A. H. Vozmediano, Phys. Rev. Lett. **69**, 172 (1992).

[6] J. González, F. Guinea, and M. A. H. Vozmediano, Nucl. Phys. B **406**, 771 (1993).

[7] S. V. Morozov, K. S. Novoselov, M. I. Katsnelson, F. Schedin, L. A. Ponomarenko, D. Jiang, and A. K. Geim, Phys. Rev. Lett. **97**, 016801 (2006).
[8] A. F. Morpurgo and F. Guinea, Phys. Rev. Lett. **97**, 196804 (2006).
[9] A. H. Castro Neto and E.-A. Kim, arXiv:cond-mat/0702562 (unpublished).
[10] The existence of corrugations implies elastic strains in the lattice (see Sec. III). Dislocations are expected on energetic grounds when the corrugations exceed a threshold value (see Sec. VI). Other topological defects, such as pentagons and heptagons which lead to declinations, are more costly energetically, although they can be formed sufficiently far from equilibrium, as shown in the growth of fullerenes and nanotubes.
[11] J. C. Meyer, A. K. Geim, M. I. Katsnelson, K. S. Novoselov, T. J. Booth, and S. Roth, Nature (London) **446**, 60 (2007).
[12] J. Sabio, C. Seoánez, S. Fratini, F. Guinea, A. H. Castro Neto, and F. Sols, Phys. Rev. B **77**, 195409 (2008).
[13] S. Cho and M. S. Fuhrer, arXiv:0705.3239 (unpublished).
[14] A. L. Vázquez de Parga, F. Calleja, B. Borca, M. C. G. Passeggi, Jr., J. J. Hinarejos, F. Guinea, and R. Miranda, Phys. Rev. Lett. **100**, 056807 (2008).
[15] A. W. W. Ludwig, M. P. A. Fisher, R. Shankar, and G. Grinstein, Phys. Rev. B **50**, 7526 (1994).
[16] C. de C. Chamon, C. Mudry, and X.-G. Wen, Phys. Rev. Lett. **77**, 4194 (1996).
[17] H. E. Castillo, C. de C. Chamon, E. Fradkin, P. M. Goldbart, and C. Mudry, Phys. Rev. B **56**, 10668 (1997).
[18] B. Horovitz and P. Le Doussal, Phys. Rev. B **65**, 125323 (2002).
[19] D. V. Khveshchenko, Phys. Rev. B **75**, 153405 (2007).
[20] D. Carpentier and P. Le Doussal, Nucl. Phys. B **588**, 565 (2000).
[21] J. Ye, Phys. Rev. B **60**, 8290 (1999).
[22] T. Stauber, F. Guinea, and M. A. H. Vozmediano, Phys. Rev. B **71**, 041406(R) (2005).
[23] I. F. Herbut, V. Juricic, and O. Vafek, Phys. Rev. Lett. **100**, 046403 (2008).
[24] D. Carpentier and P. Le Doussal, Phys. Rev. Lett. **81**, 1881 (1998).
[25] J. Martin, N. Akerman, G. Ulbricht, T. Lohmann, J. H. Smet, K. von Klitzing, and A. Yacoby, Nat. Phys. **4**, 144 (2008).
[26] H. Suzuura and T. Ando, Phys. Rev. B **65**, 235412 (2002).
[27] J. L. Mañes, Phys. Rev. B **76**, 045430 (2007).
[28] F. Guinea, J. Phys. C **14**, 3345 (1981).
[29] A. J. Heeger, S. Kivelson, J. R. Schrieffer, and W. P. Su, Rev. Mod. Phys. **60**, 781 (1988).
[30] E. Stolyarova, K. T. Rim, S. Ryu, J. Maultzsch, P. Kim, L. E. Brus, T. F. Heinz, M. S. Hybertsen, and G. W. Flynn, Proc. Natl. Acad. Sci. U.S.A. **104**, 9209 (2007).
[31] P. Le Doussal and L. Radzihovsky, Phys. Rev. Lett. **69**, 1209 (1992).
[32] J.-N. Fuchs and P. Lederer, Phys. Rev. Lett. **98**, 016803 (2007).
[33] S. Sorella and E. Tosatti, Europhys. Lett. **19**, 699 (1992).
[34] J. González, F. Guinea, and M. A. H. Vozmediano, Phys. Rev. B **63**, 134421 (2001).
[35] N. M. R. Peres, M. A. N. Araújo, and D. Bozi, Phys. Rev. B **70**, 195122 (2004).
[36] I. F. Herbut, Phys. Rev. Lett. **97**, 146401 (2006).
[37] We have also taken into account the factor of 2 misprint in σ as defined below Eq. (5) in (Ref. 24).
[38] V. L. Berezinskii, Zh. Eksp. Teor. Fiz. **61**, 1144 (1971) [Sov. Phys. JETP **34**, 610 (1972)]; J. M. Kosterlitz and D. J. Thouless, J. Phys. C **5**, L124 (1972); B. I. Halperin and D. R. Nelson, Phys. Rev. Lett. **41**, 121 (1978); D. R. Nelson, Phys. Rev. B **18**, 2318 (1978); A. P. Young, *ibid.* **19**, 1855 (1979).
[39] B. Horovitz and P. Le Doussal, Phys. Rev. B **71**, 134202 (2005).
[40] P. Le Doussal and T. Giamarchi, Physica C **331**, 233 (2000).
[41] H. S. Seung and D. R. Nelson, Phys. Rev. A **38**, 1005 (1988).
[42] Strictly, B is zero outside the core and $\vec{A}$ is a pure (singular) gauge, with correlations which diverge (Ref. 19) as $|\vec{q}|^{-2}$. A coarse grained field in the whole space can be computed (Ref. 34)—including the cores—by assigning minimal flux to each vortex (note, however, that each of these fluxes can be increased by an integer flux quantum without changing the eigenenergies while increasing the degeneracy).
[43] Due to the relation between flux and Burgers vector, the problem becomes isotropic and one may neglect the vector nature of the charges.
[44] K. I. Bolotin, K. J. Sikes, Z. Jiang, G. Fudenberg, J. Hone, P. Kim, and H. L. Stormer, arXiv:0802.2389 (unpublished).
[45] X. Du, I. Skachko, A. Barker, and E. Y. Andrei, arXiv:0802.2933 (unpublished).
[46] E. Guitter, F. David, S. Leibler, and L. Peliti, Phys. Rev. Lett. **61**, 2949 (1988); J. Phys. (France) **50**, 1787 (1989); J. A. Aronovitz, L. Golubovic, and T. C. Lubensky, *ibid.* **50**, 609 (1989).
[47] F. Guinea, G. Gómez-Santos, and D. P. Arovas, Phys. Rev. B **62**, 391 (2000).
[48] A similar estimate can be done using the magnetic field and yields the same result.
[49] F. Guinea, M. I. Katsnelson, and M. A. H. Vozmediano, Phys. Rev. B **77**, 075422 (2008).
[50] T. O. Wehling, A. V. Balatsky, M. I. Katsnelson, and A. I. Lichtenstein, arXiv:0710.5828 (unpublished).
[51] P. Esquinazi, D. Spemann, R. Höhne, A. Setzer, K.-H. Han, and T. Butz, Phys. Rev. Lett. **91**, 227201 (2003).